Vol 3 | Issue 2 | Pages 68-85

Journal of Petrochemical Engineering

Review Article

DOI: 10.36959/901/256

Pore-Throat Blocking Mechanisms in Tight Rocks by Colloidal Particles in Treated and Untreated Produced Water

Claudius Epie Njie[1], Kegang Ling[1], Olusegun Tomomewo[1], Adesina S. Fadairo[1], Luc Yvan Nkok[1], Md Jakaria[1], Abdelmalek Abes[1] and James Marti[2]*

[1]*Department of Petroleum Engineering, University of North Dakota, United States*

[2]*Physics and Nanotechnology Center, University of Minnesota, United States*

Abstract

Colloidal particles in produced water used for hydraulic fracturing can block pore throats in tight reservoir rocks through three main mechanisms. The blockage of these pore throats damages the permeability of the reservoir, leading to low productivity and higher operational cost. However, the characterization of these particles in produced water used for hydraulic fracturing is understudied. This study investigates the size distribution of these particles in produced water and the resulting pore plugging mechanisms potentially operating on typical 0.1, 0.2, and 0.4-micron-wide siltstone reservoir rock pore throats caused by primary, aggregate, and agglomerate particles in such produced waters. The siltstone pore throat diameters and particle diameters from untreated and treated produced water from McClean, McKenzie, Williams, and Mountrail Counties were compared and used to calculate the jamming ratios from which the main pore throat plugging mechanisms in those rocks were inferred. The results show that bridge blockage, and single pore blocking through straining are the main pore throat blocking mechanisms contributing to formation damage in these reservoir rocks. The bridge blocking mechanism is more prevalent when untreated produced water is used as the base fluid for hydraulic fracturing, while single pore blocking through straining is more prevalent in treated water. The size of the particles also affects the pore plugging mechanisms, with smaller particles causing damage through bridging and larger particles causing damage through single pore blockage and straining. These findings have important implications for the management of produced water in the oil and gas industry, as they may provide clues to minimize formation damage.

Keywords

Laser diffraction, Colloidal particles, Pore-throat diameter, Formation damage, Jamming ratio, Plugging mechanism

Introduction

Produced water is a byproduct of hydrocarbon extraction in the oil and gas industry, and its management is a critical aspect of operations given the large volumes involved [1]. Both solution chemistry and hydrodynamics are known to alter the permeability of porous media containing colloidal particles. Solution pH, ionic strength, and exchangeable ions determine colloid stability and hence the morphology of deposited colloids and the resulting permeability of the formation.

It has been estimated that between 10-30% of water used for the hydraulic fracturing of a well returns to the surface (Gallegos et al., 2015) [2]. This water is often contaminated with various chemicals and is laden with colloidal particles. These particles originate from uncrystallized silica, silt particles, quartz, clay particles and various oxides of iron [3]. These particles must be removed to render the water fit for injection or for hydraulic fracturing. The main benefit of this practice is to reduce the usage of fresh water, which is increasingly becoming scarce. It is desired that particles larger than 20 micrometers be eliminated from the produced water (Liden, T.; Clark, B.G.; Hildenbrand, Z.L.; Schug, K.A. 2017) before it is utilized as the base fluid in high-pressure slick

***Corresponding author:** Claudius Epie Njie, Department of Petroleum Engineering, University of North Dakota, Collaborative Energy Complex Room 113, 2844 Campus Rd Stop 8154, Grand Forks ND 58202-8153, USA

Accepted: November 29, 2023

Published online: December 01, 2023

Citation: Njie CE, Ling K, Tomomewo O, et al. (2023) Pore-Throat Blocking Mechanisms in Tight Rocks by Colloidal Particles in Treated and Untreated Produced Water. J Petrochem Eng 3(2):68-85

water hydraulic fracturing of tight reservoir rocks, to establish pathways for the flow of hydrocarbons. However, the presence and flow of colloidal particles in treated produced water in the reservoir has been shown to lead to formation damage, resulting in reduced oil and gas production [4-8]. The need to determine the potential for formation damage is therefore imperative.

Formation damage refers to the reduction in permeability and porosity of the formation, which can result in decreased flow of fluids, such as oil and gas, through the reservoir. Bennion (1999) defined formation damage in a more succinct manner as "The impairment of the invisible by the inevitable and uncontrollable, resulting in an indeterminate reduction of the unquantifiable" Formation damage can be caused by a variety of factors [6], including the injection of incompatible fluids or a suspension of solid material most of which cannot be easily removed economically. As a result, colloidal particles persist in water that has been treated for reuse as base fluid for hydraulic fracturing. In terms of size, these particles are in the micron range and compare with the pore-throat size ranges found in tight reservoir rocks in the middle Bakken and other unconventional shale formations. The presence of such suspended particles in treated produced water has been identified as a potential cause of formation damage, as these particles can clog pores and reduce the effective permeability of the formation [9-11]. Hence the need to characterize them. The permeability reduction in the reservoir is a result of both the attachment and retention of particles on pore wall and pore throats respectively [12]. Attachment to these pore walls is achieved by strong electrostatic forces.

Trapping mechanisms

Particle migration toward pore throat constrictions during hydraulic fracturing is driven by thermal energy and mechanical agitation. This migration influences the critical retention concentration, which distinguishes particles held within pore throats from those that escape. Importantly, the passage of particles through pore throats reduces fluid flow permeability in the rock formation [13].

Colloidal particles are retained in the smallest compartments of the pore space through the process of straining [14-18]. The tightness of these spaces causes fluid velocity restriction to the point of stagnation, where fluids cannot flow, resulting in stagnation zones. In these zones, particles become trapped, reduce the permeability of the formation and consequently impeding hydrocarbon flow.

Stagnation zones can be formed in pores when the hydraulic fracturing process has been terminated and the well closed for pressure build-up. In this case, the hydrodynamic force from the fluid that may cause dislodging of strained and retained particles in the pores is non-existent and the particles are held permanently in the pore space by electrical forces, van der Waals forces, sorption, and gravitational force (Figure 1).

The straining of these colloidal particles through single pore throats is a function of the ratio of particle diameter to the pore size distribution of the rock (Herzig et al., 1970) [14,16,17].

In 1970, Herzig et al. [14] reported that, when $\frac{diameter\ of\ \ pore\ throat\ (dt)}{diameter\ of\ the\ particle\ (dp)} > 0.05$, single pore blocking of particles by straining into the pore space is the dominant retention mechanism of particles within the porous medium. This ratio can reduce to 0.02 for single pore blockage via straining to still dominate the retention of particles in the porous media [16,20]. The ratios of pore throat diameter to particle diameter reported by Herzig, et al. is the Jamming ratio, J. When the jamming ratio is out of the ranges defined by Herzig, et al. and Bradford, et al., pore blockage through bridging is the dominant mechanism.

If the initial permeability K_0 of the formation is known, and the permeability reduction of the formation after formation damage by particle retention and straining is equally known $\left(K_O\right)$, the percentage reduction in permeability can be expressed mathematically as

$$\frac{K\left(\alpha\right)}{K_O} = \frac{1}{1+\beta\left(1-\alpha_{cr}\right)}$$

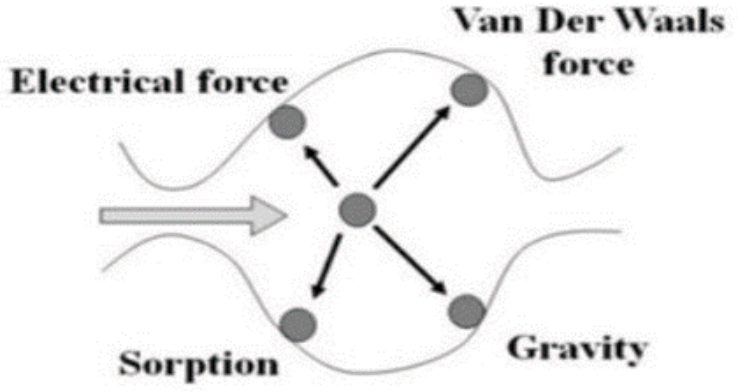

Figure 1: Forces retaining colloidal particle in pore space in stagnation zone [19].

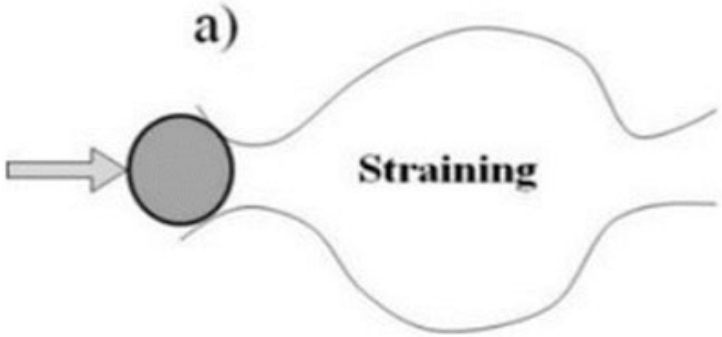

Figure 2: Single pore blocking via straining [19].

Figure 3: Bridge plugging mechanism [19].

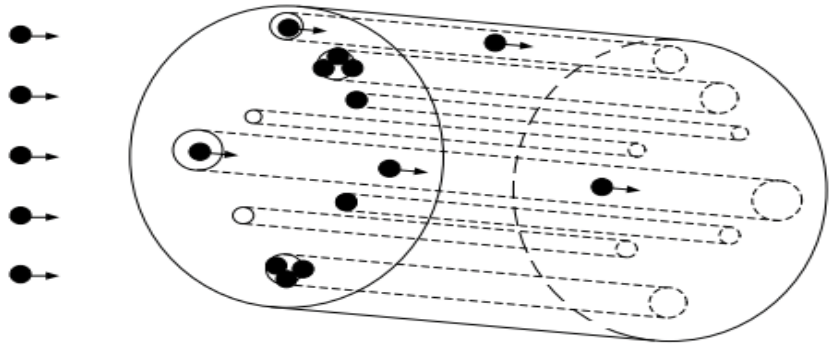

Figure 4: Single and bridged pore throat blockage [23].

where α_{cr} is the critical retention concentration of particles, and β is the formation damage coefficient.

Single pore blocking: If the sizes of the colloidal particles in the produced water are comparable or bigger than the size of the pore-throats, single pore blocking occurs according to the straining rules of Herzig, et al., and Bradford, et al. (Figure 2).

Bridge Blockage: The bridge blocking pore throat mechanism involves the blockage of pore throats, by curved bridges of several small particles, each of which has a diameter smaller than the pore throat [21]. The particles agglomerate via electrostatic forces of attraction and the resulting bridge partially or completely blocks the pore-throat (Figure 3).

Single pore blocking and bridging blocking are thus regarded as the main pore-throat blockage mechanisms in both conventional and unconventional reservoir rocks. The operational prevalence of each blocking mechanism is contingent upon the dispersion pattern of colloidal particles present in the utilized fracking-produced water. Although these two mechanisms operate autonomously, they may concomitantly manifest under certain circumstances [22] (Figure 4).

In this study, we aim to characterize the colloidal/suspended particles in treated produced water used for hydraulic fracturing. Water samples were obtained from four counties (Williams, Mountrail, McKenzie & McClean) in which there is considerable hydrocarbon production through

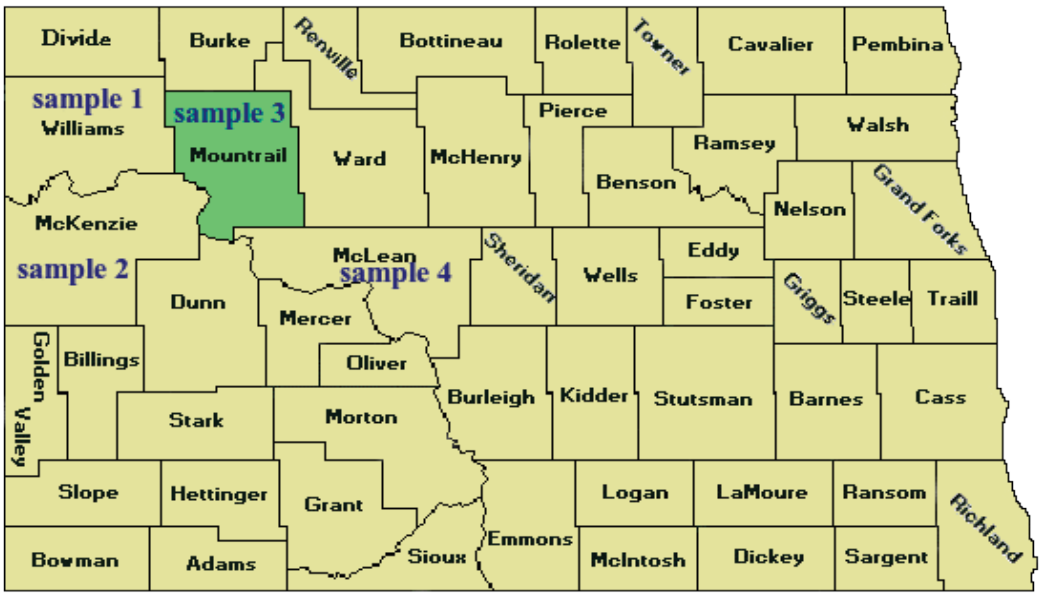

Figure 5: North Dakota Oil producing Counties from which Samples of treated & untreated produced water were obtained for this study (Map-Courtesy: North Dakota Geological Survey).

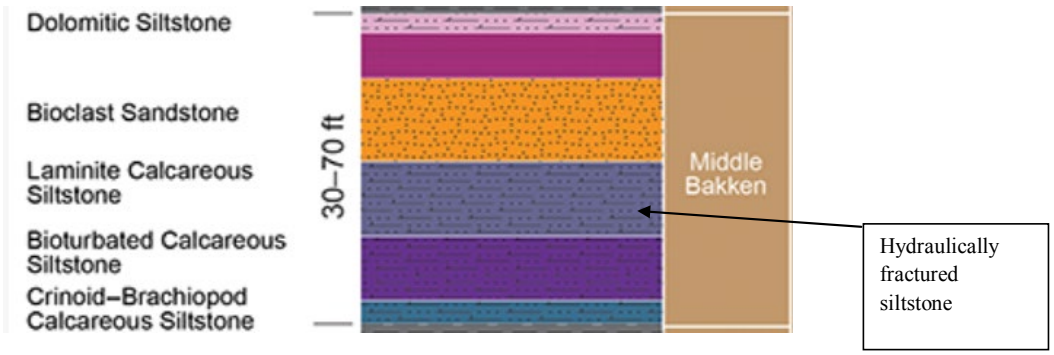

Figure 6: Lithology of Middle section of the Bakken.

hydraulic fracturing. Specifically, it is desired to determine the pore throat blocking mechanisms by colloidal particles on pores of a typical Middle Bakken laminite calcareous siltstone producing reservoir. The Source of these samples are shown in Figure 5.

Geological Setting of the Williston Basin

The United States' Williston Basin, which includes sections of Montana, North Dakota, South Dakota, and Wyoming, is a major hydrocarbon-producing area. The Three Forks Formation, which in eastern McKenzie County has a maximum thickness of 250 feet, lies beneath the Bakken. Shales, dolostones, siltstones, sandstones, and traces of anhydrite are among the rocks that make up the Three Forks Formation. These rocks serve as the primary reservoirs from which hydraulic fracturing is applied to produce hydrocarbons (Figure 6). The pore-throat size ranges from a few nanometers to several microns.

Shales are high clay content reservoir rocks inherently susceptible to formation damage [24-26]. Understanding the interaction between siltstones and the colloidal particles in produced waters used for hydraulic fracturing is important for developing effective strategies for reducing the impact of pore throat blocking and the extent of formation damage this can produce. To achieve our objectives, laser diffraction technique was used for colloidal particle size characterization [27]. This methodology facilitates precise quantification of the size distribution of such colloidal particles within treated/untreated produced water employed in hydraulic fracturing, enabling the assessment of their propensity to obstruct pore-throats by comparing their sizes with the characteristic pore-throat dimensions of a siltstone reservoir layer. A Jamming ratio was calculated from pore throat sizes of 0.1, 0.2 and 0.4 microns prevalent in a typical laminite calcareous siltstone reservoir rock (Figure 6) and from this ratio, the dominant pore throat blocking mechanisms that can potentially cause formation damage were determined.

Materials & Methods

- Filtered but untreated produced water samples were

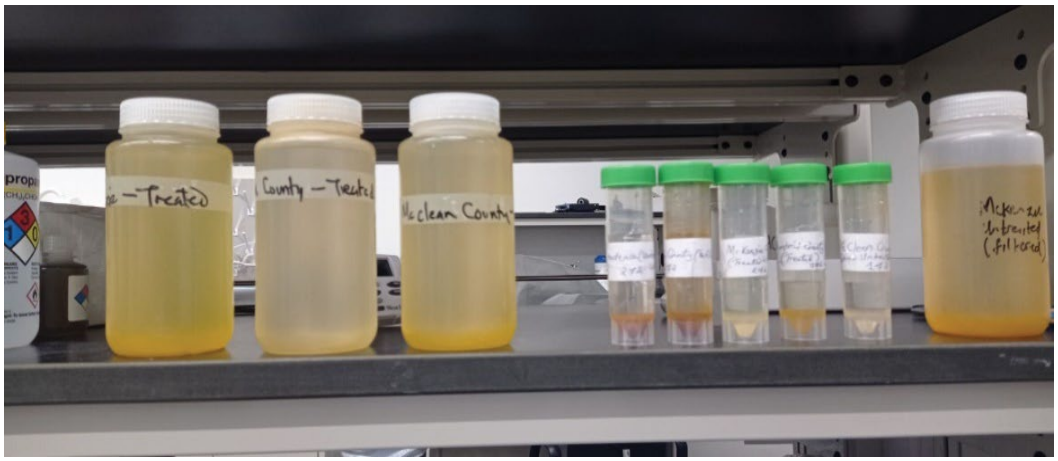

Figure 7: Produced Water samples from the WMMM (**Sample 1,2,3,4**) Counties in Williston Basin.

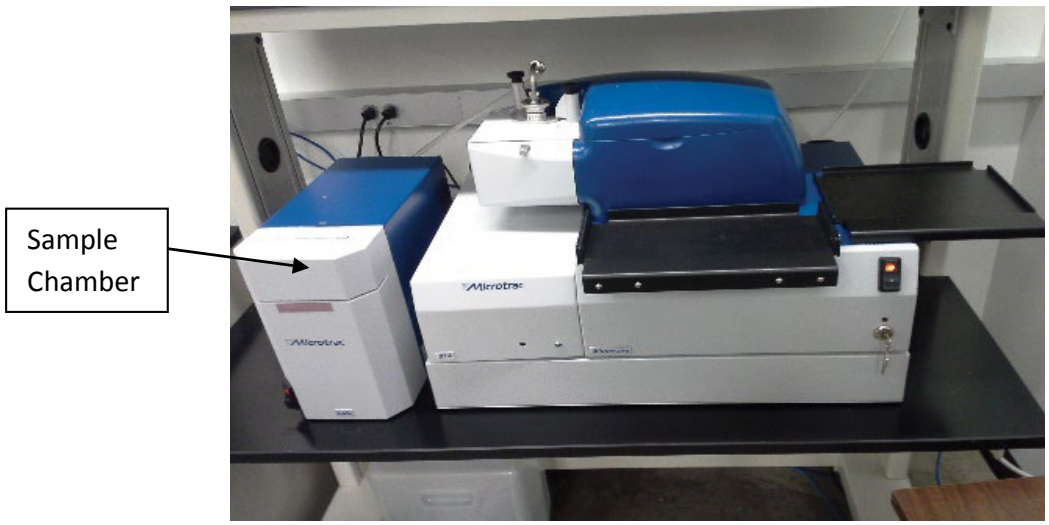

Figure 8: BlueWave Laser Diffraction particule Analyzer (Courtesy: Microtrac).

obtained from Williams County, McClean County, Mountrail County, and McKenzie Counties in the Williston Basin (WMMM)

- Filtered and treated produced water samples were also obtained from the same counties (see Figure 7 below).

Methodology

The colloidal particle Size Measurement and distributions of the produced water samples was determined by the Laser Diffraction Particle Analyzer known as the BlueWave (manufactured by Microtrac). This is shown in Figure 8.

Principle and Tool description: The principle behind laser diffraction is that the diffraction pattern produced by a group of particles is directly related to the size distribution of the particles. When a laser beam is shone through a sample containing particles, the particles scatter the light in all directions. The diffraction pattern produced by this scattering is a series of bright and dark bands, known as fringes. These resulting fringes are caused by constructive and destructive interference of the scattered light waves. The spacing of the fringes is related to the size of the particles. Larger particles produce wider spacing between the fringes and small particles produce a comparatively narrower spacing between the fringes. Upon analysis of this diffraction pattern, the size distribution of the particles in the sample is determined.

For this investigation, the Microtrac BlueWave laser diffraction particle size analyzer was used to determine the particle sizes of the suspended particles in each of the produced water samples and their corresponding size distributions. The instrument was chosen primarily due to its extensive measurement range, versatility, and ability to process a high number of samples and for its good reproducibility of the results obtained as required by the ISO 13320-2020 standard for measurement of particle size by laser diffraction. A schematic diagram showing the optical layout of the instrument used for all the measurements in this investigation is shown in Figure 9.

The BlueWave is a particle characterization tool that uses the light diffracted by suspended particles to derive their

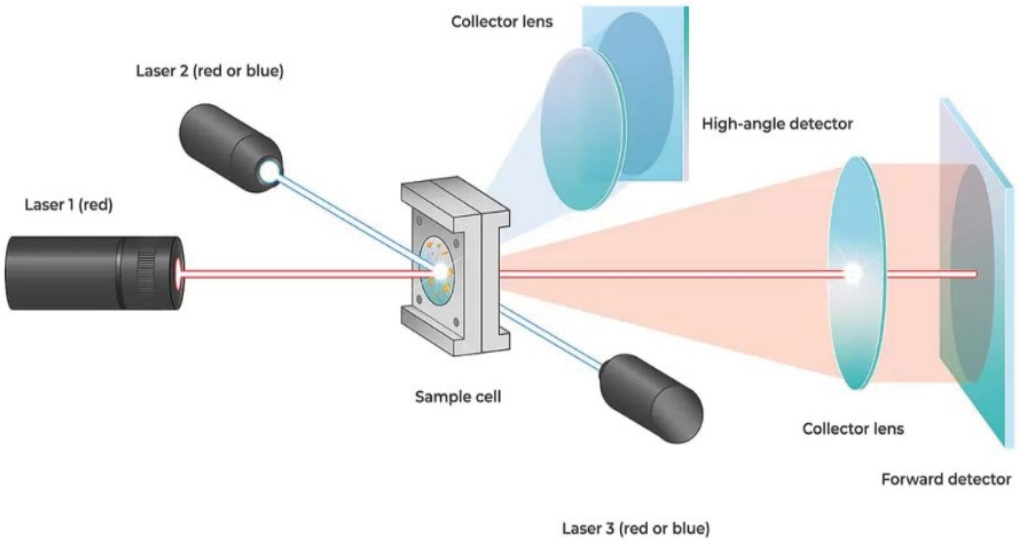

Figure 9: (Microtrac MRB, www.microtrac.com/products/particle-size-shape-analysis/laser-diffraction).

Table 1: Standard operating procedure (for the BlueWave with water as circulating fluid).

Settings	Parameter
Measurement time per sample	15 seconds
Flow rate of circulating fluid	70
Number of Rinses of sample chamber before new measurement	4
Number of times measurement is taken	3

size distribution. The BlueWave is capable of particle size measurements ranging from 50 nm to 2800 microns. The system suspends the particles in a liquid and circulates the suspension through an optical cell. In this optical cell, lasers of three different wavelengths strike the sample. The light produced by these lasers is diffracted by an ensemble of particles in the sample, and a diffraction pattern is produced. The maxima and minima of the combined diffraction patterns of these particle ensembles are then recorded by detectors. An inversion algorithm is used to separate the pattern created by each particle in the ensemble, and the system software calculates the particle size distribution based on these diffraction patterns.

Measurement procedure: The instrument was set up for measurements according to the standard operating procedure (SOP) in Table 1 in compliance with the ISO 13320-2020 standard in step 1, and the measurements were taken in steps 2, 3 and 4.

Step 1

Table 1

Step 2

In compliance with ISO 13320 - 2020, the sample chamber was rinsed four times, and the instrument was put into the circulation mode. A representative portion of the produced water was agitated and methodically dispensed into the instrument's sample chamber in a drop wise manner until the particle sensor detected a signal, indicating that the measurement process could commence.

Step 3

Following detection of this signal, the "measure" command in the operation software panel was activated, causing the instrument to acquire the particle size distribution. In accordance with standard operating procedure in Table 1 above, the measurement of particle size distribution was automatically repeated three times by the instrument, and the average particle size distribution was subsequently determined in volume mode.

Step 4

The instrument was then engaged to the rinse mode and the already analyzed sample is drained out of the instrument and the sample chamber rinsed four times as programmed in the SOP in Table 1. The next sample was then introduced into the instrument and the same procedure as in step 2 above is repeated to obtain the particle size distribution for all the produced water samples.

Results & Discussion

The size distribution of the colloidal particles in the untreated and treated produced water samples from the listed counties in the Williston Basin were measured by the Blue Wave Laser Diffraction tool in accordance with the standard operating procedure. To obtain the distributions, three separate measurements of the particle size distribution

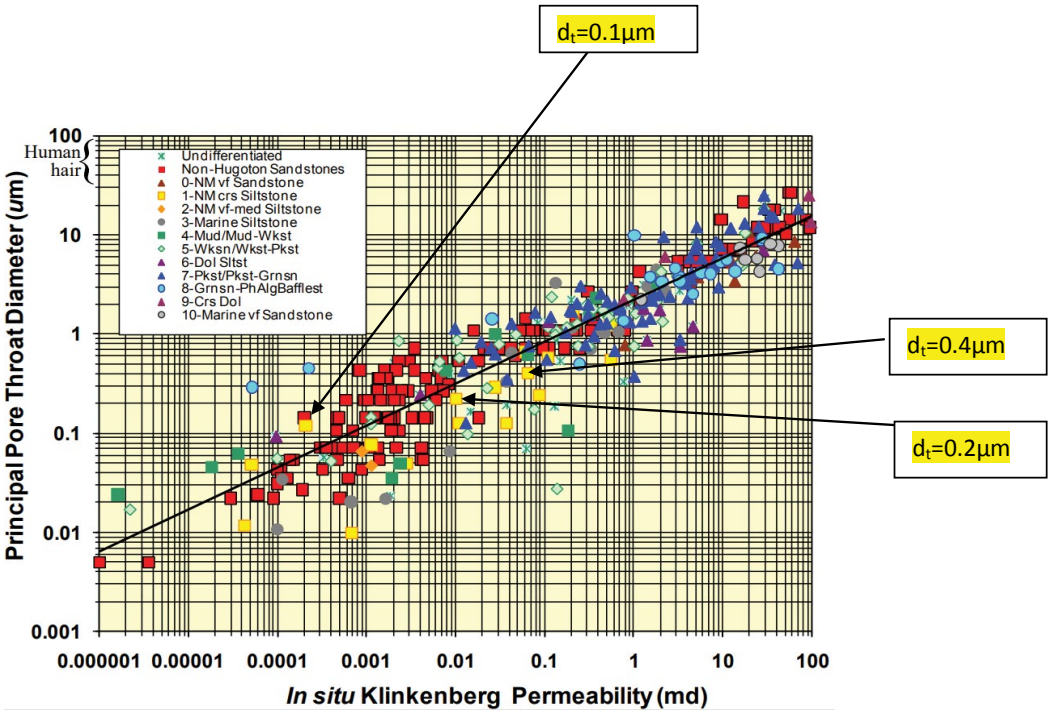

Figure 10: Relationship between Pore throat diameter of different lithologies and In-situ Klinkenberg permeability (after Byrnes, 2009) [28].

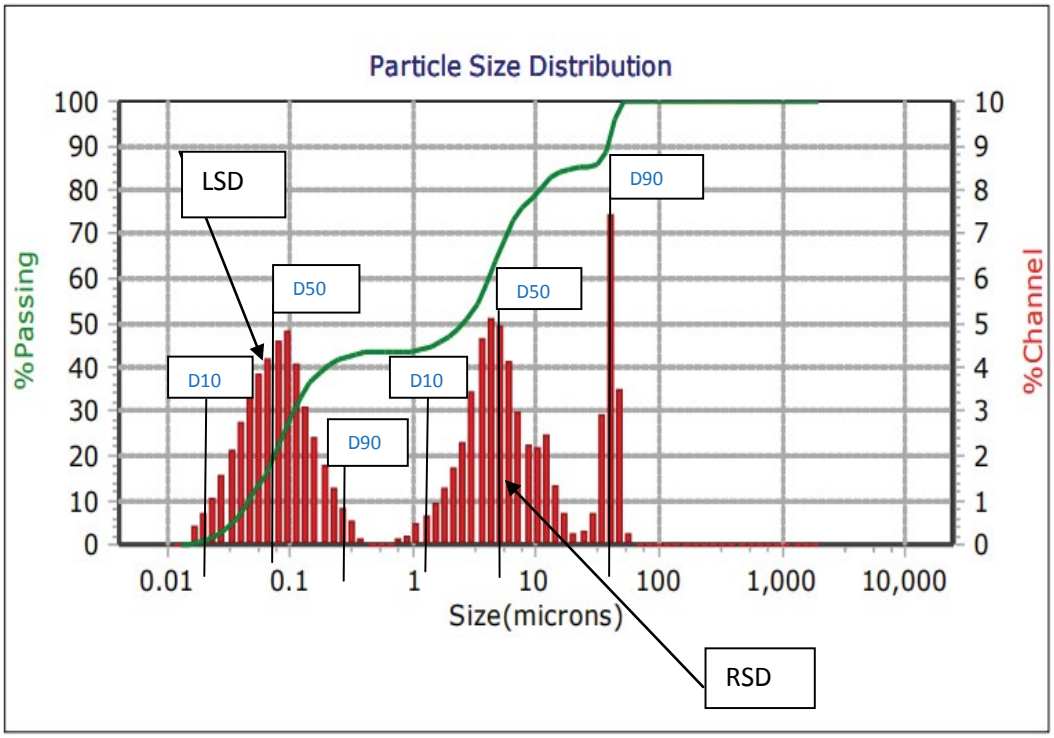

Figure 11: Particle Size distribution of Treated McClean Produced Water. It is a bimodal distribution with a left side distribution (LSD) and right-side distribution (RSD) each of which have distinct values for D10, D50 and D90.

for each sample was obtained and averaged. So, Figure 10, Figure 11, Figure 12, Figure 13, Figure 14, Figure 15 and Figure 16 are average particle size distributions obtained for each sample after conducting the measurement three times to reduce the measurement error.

The pore throat sizes for a typical representative siltstone,

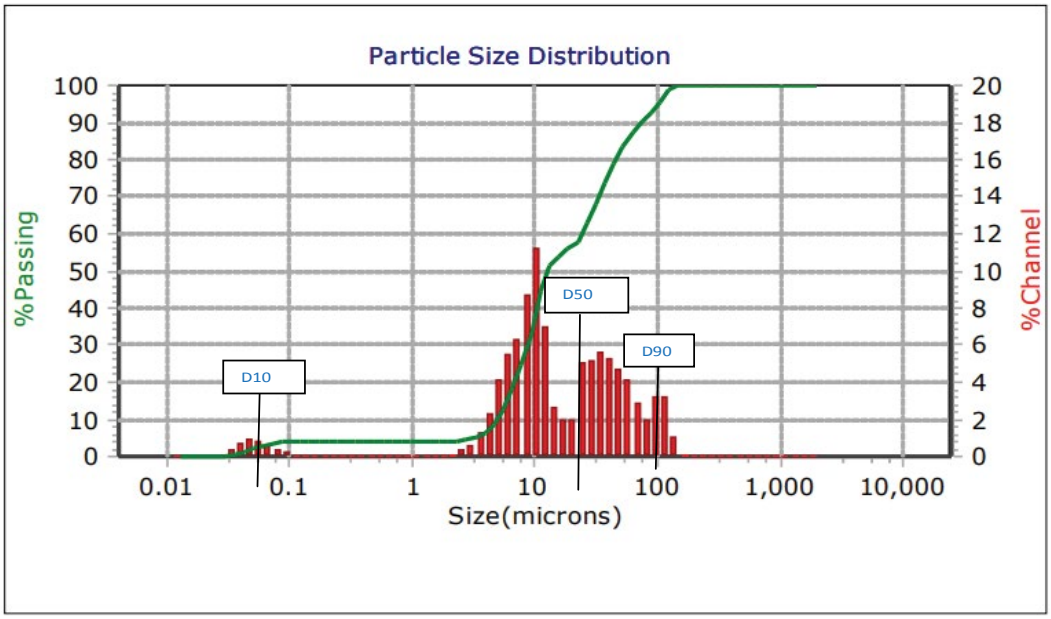

Figure 12: Particle size distribution for McKenzie Untreated filtered Produced Water.

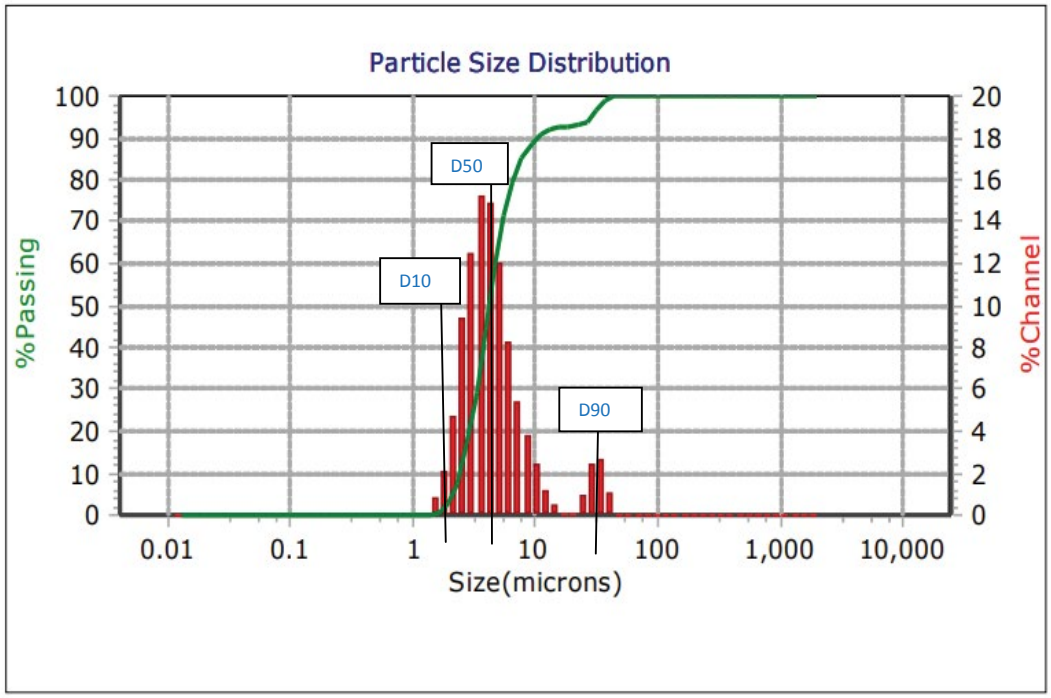

Figure 13: Particle size distribution for McKenzie treated Filtered Produced Water.

such as those found within the middle Bakken, were obtained by reading them off the graph from experimental work performed by Byrnes, et al., [28] (see Figure 10).

McClean County produced water particle size distribution results

As shown in Figure 10, the size range of the particles in the untreated samples from the McClean County was found to be between 3 and 10 microns. This means that from this narrow distribution primary particles measure around 3 microns. When these particles aggregate, the spherical diameter reaches 50 microns. Agglomeration of the particles produces particle composites measuring about 10 microns in diameter. The primary particles are likely to block the pore throats by the bridging mechanism and reduce the permeability of the formation by particle straining and retention (Table 1a).

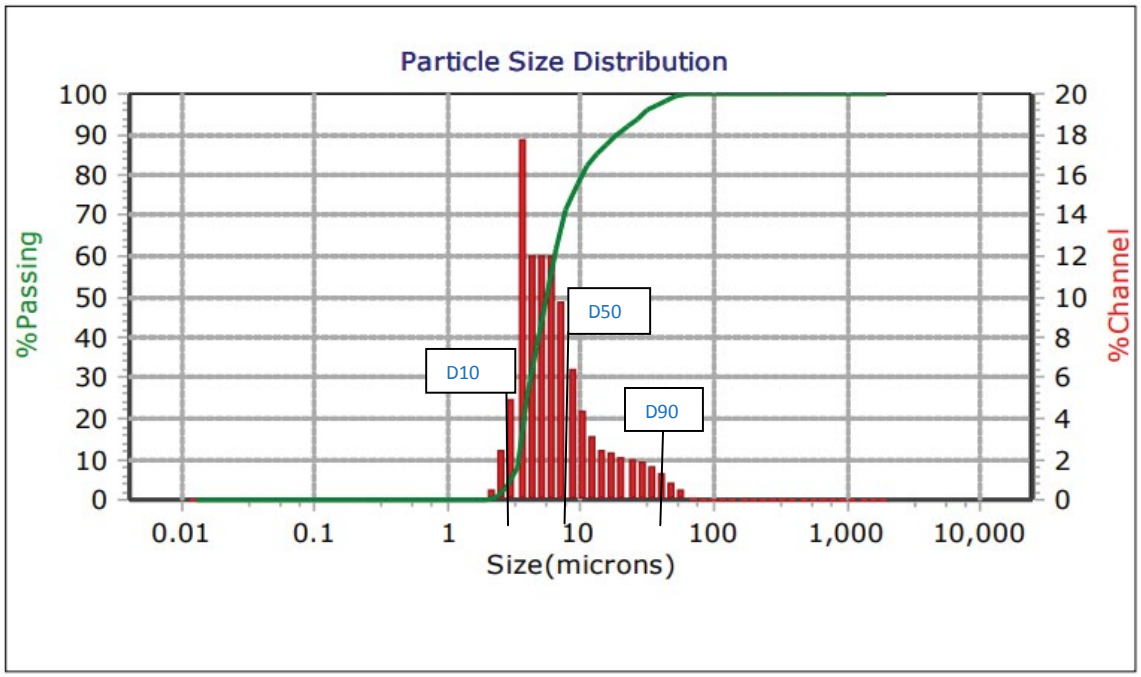

Figure 14: Particle size distribution for Williams County Untreated produced water.

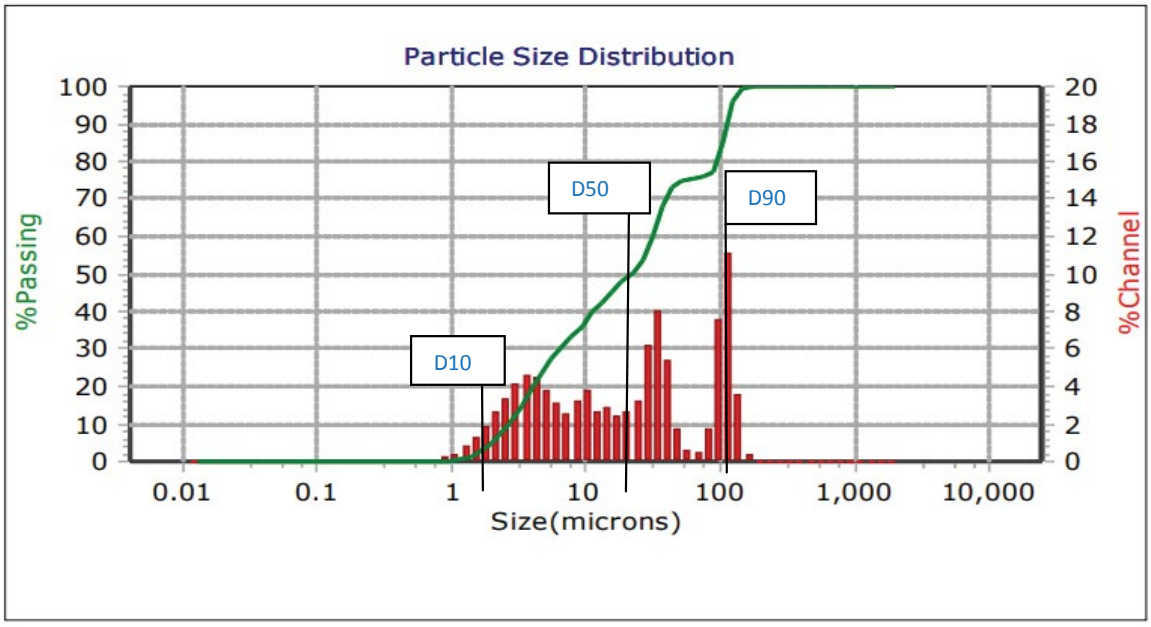

Figure 15: Particle size distribution for treated Williams County Produced Water.

The particle size distribution statistics displayed in Table 2 above provides information on the particle sizes but does not include information on aggregation and agglomeration of the particles. Since the distributions are skewed, it is assumed that single or primary particles measure at the D10 position of the distribution graph. Owing to the charged nature of these particles, aggregates and agglomerates are formed and measure at the D50 and D90 positions of the plot respectively. In the table above the actual D50 used in Jamming ratio calculations cannot be 31.09 microns. It is rather 5 microns. Aggregates are assumed to measure about 4 microns on average. This is the reasoning behind all the particle size distribution graphs in this work.

Based on the jamming ratios in Table 1b above, it can be inferred that the main pore blocking mechanism capable of causing formation damage by primary and aggregate particles is the single blockage mechanism through straining. Agglomerates block pore throats by bridging mechanism.

It can be inferred from the jamming ratios in Table 1c

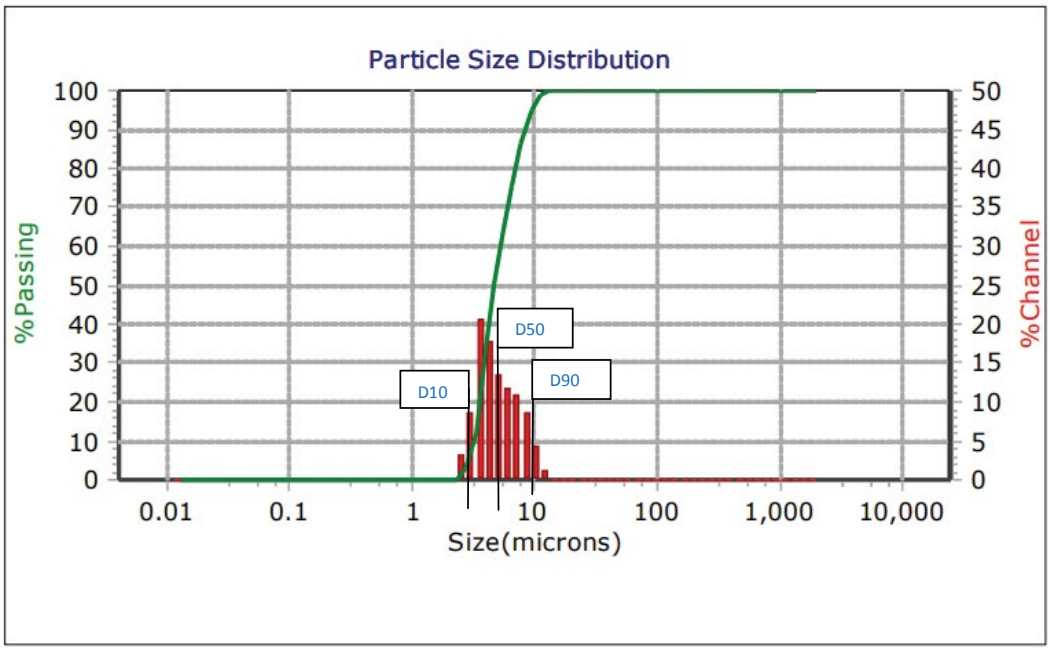

Figure 16: Particle size distribution for Mountrail County treated produced water.

Table 1a: Particle size distribution statistics for McClean Untreated produced water.

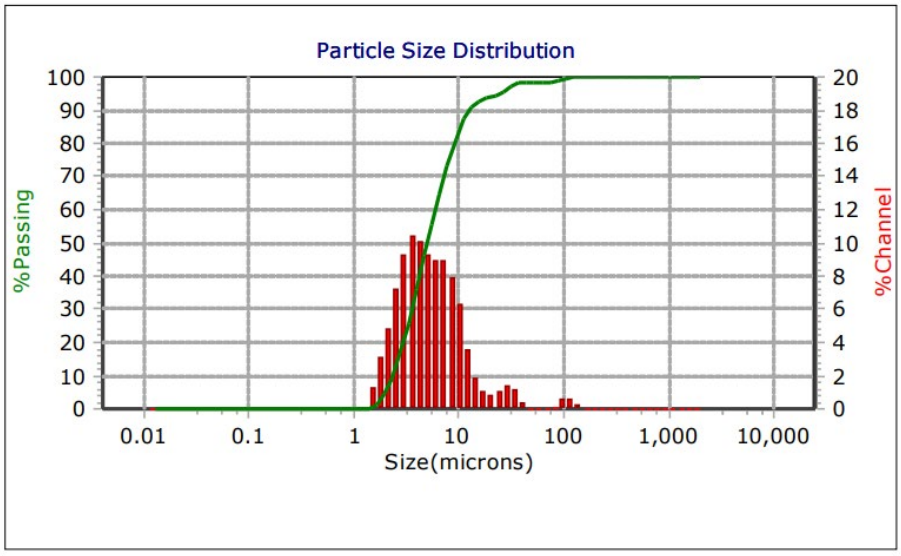

Table 1b: Jamming Ratio for particles in untreated McClean Produced Water on siltstone with d_t = 0.1.

	Pore-throat diameter(d_t) (in microns)	**Particle diameter(d_p) (in microns)**	$J = d_t / d_p$
Primary particle (D10)	0.1	2	0.05
Aggregate (D50)	0.1	4	0.025
Agglomerate (D90)	0.1	45	0.0022

above that, pore throat blockage is caused by primary and aggregate particles by the single pore blockage mechanism through straining. The agglomerates block pore through throats by the bridging mechanism.

From Table 1d above, it can be inferred from the jamming ratios that all particles penetrate and block the pore space through the single pore blocking mechanism through straining. Meanwhile, the agglomerates block the pore throats by the bridging mechanism.

The algorithm used in plotting the particle size distribution determines the particle statistical parameters as though the distribution was unimodal. In this case however, there are

Table 1c: Jamming Ratio for particles in untreated McClean Produced Water on siltstone with d_t = 0.2.

	Pore-throat diameter (d_t) (in microns)	**Particle diameter(d_p) (in microns)**	d_t/d_p
Primary particle (D10)	0.2	2	0.05
Aggregate (D50)	0.2	4	0.05
Agglomerate (D90)	0.2	45	0.0044

Table 1d: Jamming Ratio for particles in untreated McClean produced water on siltstone with d_t = 0.4.

	Pore-throat diameter (d_t) (in microns)	**Particle diameter (d_p) (in microns)**	d_t/d_p
Primary particle (D10)	0.4	2	0.2
Aggregate (D50)	0.4	4	0.1
Agglomerate (D90)	0.4	45	0.0089

Table 2: Particle size distribution statistics for McClean untreated produced water.

Statistic	**Value**
MV (µm)	31.09
MN (µm)	3.22
MA (µm)	8.20
CS	7.31 exp (-1)
SD	1.290
M_z	36.30
ϭ1	40.18
Ski	0.873
Kg	1.793

Table 2a: Particle Size distribution Statistics for McClean Treated Produced Water.

Parameter	**Value**
MV (µm)	8.74
MN (µm)	0.0320
MA (µm)	0.1410
CS	42.44
SD	7.60
M_z	5.98
ϭ1	10.26
Ski	0.773
Kg	2.412

Table 2b: Jamming Ratio for particles in treated McClean produced water on siltstone with d_t = 0.1 micron for LSD.

	Pore-throat diameter(d_t) (in microns)	**Particle diameter(d_p) (in microns)**	d_t/d_p
Primary particle (D10)	0.1	0.03	3.33
Aggregate (D50)	0.1	0.09	1.11
Agglomerate (D90)	0.1	0.47	2.13

Table 2c: Jamming Ratio for particles in treated McClean produced water on siltstone with d_t = 0.2 micron for LSD.

	Pore-throat diameter (d_t) (in microns)	**Particle diameter (d_p) (in microns)**	d_t/d_p
Primary particle (D10)	0.2	0.03	6.66
Aggregate (D50)	0.2	0.09	2.22
Agglomerate (D90)	0.2	0.47	0.425

Table 2d: Jamming Ratio for particles in treated McClean produced water on siltstone with d_t = 0.4.

	Pore-throat diameter (d_t) (in microns)	**Particle diameter (d_p) (in microns)**	d_t/d_p
Primary particle (D10)	0.4	0.03	13.33
Aggregate (D50)	0.4	0.09	4.44
Agglomerate (D90)	0.4	0.47	0.851

Table 2e: Jamming Ratio for particles in treated McClean produced water on siltstone with d_t = 0.1 micron for RSD.

	Pore-throat diameter (d_t) (in microns)	**Particle diameter (d_p) (in microns)**	d_t/d_p
Primary particle (D10)	0.1	0.03	3.33
Aggregate (D50)	0.1	0.09	1.11
Agglomerate (D90)	0.1	0.47	2.13

Table 2f: Jamming Ratio for particles in treated McClean produced water on siltstone with d_t = 0.2 micron for RSD.

	Pore-throat diameter (d_t) (in microns)	**Particle diameter (d_p) (in microns)**	d_t/d_p
Primary particle (D10)	0.2	0.03	3.33
Aggregate (D50)	0.2	0.09	1.11
Agglomerate (D90)	0.2	0.47	2.13

Table 2g: Jamming Ratio for particles in treated McClean produced water on siltstone with d_t = 0.4 micron for RSD.

	Pore-throat diameter (d_t) (in microns)	**Particle diameter (d_p) (in microns)**	d_t/d_p
Primary particle (D10)	0.4	0.03	3.33
Aggregate (D50)	0.4	0.09	1.11
Agglomerate (D90)	0.4	0.47	2.13

Table 3: Particle size distribution statistics McKenzie Untreated filtered produced water.

Parameter	**Value**
MV (micron)	28.15
MN (micron)	0.0410
MA (micron)	1.081
CS	5.55
SD	23.73
M_z	24.08
Ϭ1	26.78
Ski	0.770
Kg	1.301

two distinct distributions of particles that have been handled separately (Table 2a).

Based on the Jamming ratios in Table 2b, it can be inferred that all the particles block pore throats of this size via the single pore blocking mechanism.

Based on the Jamming ratios in Table 2c, it can be inferred that through pore throat sizes of 0.2-micron, all the primary particles, aggregates and agglomerates block the pores through single pore blocking mechanism.

The bimodal nature of the particle size distribution is an indication that suspended colloidal particles have and could be broken down into smaller size ranges by mechanical agitation. The implication here is that the propensity for the particles to block pore throats may become higher since the agitation of the particles by high pressure hydraulic fracturing fluid may decrease their size below the 1 µm – 10 µm size range (Table 2d).

For the RSD, the Jamming ratios were also determined as shown in Table 2e and Table 2f.

From the Table 2e, it can be inferred that the single pore blockage is the dominant mechanism at this pore throat diameter.

Also from the Table 2f, it can be inferred that the single pore blockage is the dominant mechanism at this pore throat diameter.

Table 3a: Jamming Ratio for particles in untreated McKenzie produced water on siltstone with d_t = 0.1.

	Pore-throat diameter (d_t) (in microns)	**Particle diameter (d_p) (in microns)**	d_t/d_p
Primary particle (D10)	0.1	0.08	1.25
Aggregate (D50)	0.1	40	0.0025
Agglomerate (D90)	0.1	100	0.001

Table 3b: Jamming Ratio for particles in untreated McKenzie produced water on siltstone with d_t = 0.2.

	Pore-throat diameter (d_t) (in microns)	**Particle diameter (d_p) (in microns)**	d_t/d_p
Primary particle (D10)	0.2	0.08	2.5
Aggregate (D50)	0.2	40	0.005
Agglomerate (D90)	0.2	100	0.002

Table 3c: Jamming Ratio for particles in untreated McKenzie Produced Water on siltstone with d_t = 0.4.

	Pore-throat diameter (d_t) (in microns)	**Particle diameter (d_p) (in microns)**	d_t/d_p
Primary particle (D10)	0.4	0.08	5.00
Aggregate (D50)	0.4	40	0.01
Agglomerate (D90)	0.4	100	0.004

Table 3d: Particle size distribution statistics McKenzie treated Filtered Produced Water.

Parameter	**Value**
MV (µm)	6.44
MN (µm)	2.79
MA (µm)	4.00
CS	1.501
SD	2.398
M_z	4.79
Ϭ1	5.20
Ski	0.628
Kg	3.86

Similarly in Table 2g, it can be inferred that the single pore blockage is the dominant mechanism at this pore throat diameter.

McKenzie County particle size distribution results

In the case of untreated but filtered produced water from McKenzie County, the particle size distribution is unimodal and broad, with particles measuring in the 10 micron - 100 micron size range. The distribution is negatively skewed, indicating, and confirming the high percentage of fine primary particles in the 0.1 micron - 1 micron size range.

From the jamming ratios in Table 3a, it can be inferred that blockage occurs through single pore blockage by straining of primary particles through 0.1-micron pore throats. However, most of the blockage is caused by the aggregate and agglomerates by bridging mechanism.

For 0.2 micron pore throats Table 3b, it can be inferred, based on the Jamming ratios in Figure 3b above that, primary particles block pore throats through the single pore blocking mechanism through straining However, the aggregates and agglomerates contribute to this blocking via the bridge blocking mechanism.

For 0.4 micron pore throats Table 3c, it can be inferred, based on the Jamming ratios in Figure 3c above that, primary particles block pore throats through the single pore blocking mechanism through straining. However, the aggregates and agglomerates contribute to this blocking via the bridge blocking mechanism.

Based on the Jamming ratio in Table 3d and Table 3e, it can be inferred that, through 0.1-micron pore throats in a typical siltstone reservoir rock, the primary particles strain through the pore throats to cause blockage by the single blockage mechanism. The aggregates and agglomerates all block the pore space through the bridging mechanism.

Based on the Jamming ratios in Table 3f, it can be inferred that, primary particles, and the aggregates, block the pore space through the single blocking mechanism through straining across the 0.2-micron pore throats. However, the agglomerates block the pore throats via the bridge mechanism.

At pore throat size of 0.4 micron, the jamming ratios in

Table 3e: Jamming Ratio for particles in treated McKenzie produced water on siltstone with d_t = 0.1

	Pore-throat diameter (d_t) (in microns)	Particle diameter (d_p) (in microns)	d_t/d_p
Primary particle (D10)	0.1	3	0.033
Aggregate (D50)	0.1	6	0.0166
Agglomerate (D90)	0.1	50	0.002

Table 3f: Jamming Ratio for particles in treated McKenzie produced water on siltstone with d_t = 0.2

	Pore-throat diameter (d_t) (in microns)	Particle diameter (d_p) (in microns)	d_t/d_p
Primary particle (D10)	0.2	3	0.066
Aggregate (D50)	0.2	6	0.033
Agglomerate (D90)	0.2	50	0.004

Table 3g: Jamming Ratio for particles in treated McKenzie produced water on siltstone with d_t = 0.4.

	Pore-throat diameter(d_t) (in microns)	Particle diameter(d_p) (in microns)	d_t/d_p
Primary particle (D10)	0.4	3	0.133
Aggregate(D50)	0.4	6	0.066
Agglomerate(D90)	0.4	50	0.04

Table 4: Particle size distribution statistics for Williams County untreated produced water.

Parameter	Value
MV (µm)	8.65
MN (µm)	3.82
MA (µm)	5.41
CS	1.109
SD	4.28
M_z	7.07
Ϭ1	6.05
Ski	0.675
Kg	2.288

Table 3g above suggest that all the particles block the pore throats through the single pore blocking mechanism.

Williams county produced water

Untreated produced water from the Williams County shows a broad distribution with microparticles measuring in the 5-90 µm size range. The distribution is positively skewed confirming the presence of a higher proportion of larger particles than smaller particles within this size range.

The jamming ratios in Table 4a suggest that blockage of the 0.1-micron throats of siltstone reservoir rocks pore throats is caused by the primary particles via the single pore blockage mechanism. The aggregates and agglomerates block the pore throats via the bridge blocking mechanism.

From the Jamming ratios in Table 4b, it can be inferred that both the primary and aggregate particles block the pores by the single pore blockage mechanism through straining. The agglomerates block the pore space through the bridge mechanism across the all 0.2-micron pore throats.

Looking at the Jamming ratios in Table 4b, it can be inferred that both the primary and aggregate particles block the pores by the single pore blockage mechanism through straining. The agglomerates block the pore space through the bridge mechanism across the all 0.4-micron pore throats (Table 4c).

From the values of the jamming ratios in Table 4d and Table 4e, it can be inferred that only bridging blockage is the main pore blocking mechanism for primary particles, aggregates, and agglomerates at the pore throat size of 0.1 micron.

At a pore throat size of 0.2 micron Table 4f, it can be inferred from the jamming ratios in Table 4g that the primary particles block the pore throats by the single pore blocking mechanism. Meanwhile, the aggregates block the pores by the bridging mechanism.

At a pore throat size of 0.4 micron, it can be inferred from the jamming ratios in Table 4g that the primary particles block the pore throats by the single pore blocking mechanism. The aggregates block the pores by the bridging mechanism.

Mountrail county produced water

Treated produced water from the Mountrail County shows

Table 4a: Jamming Ratio for particles in Williams County untreated produced water on siltstone with d_t = 0.1.

	Pore-throat diameter (d_t) (in microns)	**Particle diameter (d_p) (in microns)**	$J = d_t / d_p$
Primary particle (D10)	0.1	3	0.033
Aggregate (D50)	0.1	10	0.01
Agglomerate (D90)	0.1	70	0.001

Table 4b: Jamming Ratio for particles in Williams County untreated produced water on siltstone with d_t = 0.2.

	Pore-throat diameter (d_t) (in microns)	**Particle diameter (d_p) (in microns)**	d_t / d_p
Primary particle (D10)	0.2	3	0.06
Aggregate (D50)	0.2	10	0.02
Agglomerate (D90)	0.2	70	0.003

Table 4c: Jamming Ratio for particles in Williams Cty untreated produced water on siltstone with d_t = 0.4.

	Pore-throat diameter (d_t) (in microns)	**Particle diameter (d_p) (in microns)**	d_t / d_p
Primary particle (D10)	0.4	3	0.133
Aggregate (D50)	0.4	10	0.04
Agglomerate (D90)	0.4	70	0.006

Table 4d: Particle size distribution statistics for treated Williams County Produced Water.

Parameter	**Value**
MV (µm)	39.03
MN (µm)	1.883
MA (µm)	7.45
CS	8 exp (-1)
SD	49.74
M_z	42.60
б1	43.08
Ski	0.658
Kg	0.961

a very narrow distribution of fine particles measuring in the 5 µm - 8 µm size range. The percentage of particles lower than 5 microns was characteristically small and this water appeared to meet the requirements for injection and for usage as hydraulic fracturing fluid. However, the possibility of pore throat blockage cannot be totally excluded since the pore throats of large pores can be blocked.

From the Jamming ratio in Table 5a, it can be inferred that only the primary particles bridge pore throats of this size and cause blockage. Aggregates and agglomerates block pore throats by the single pore blockage mechanism through straining.

With pore throat sizes of 0.2-micron, it can be inferred from the jamming ratio that blockage of pore throats by primary particles, aggregates and agglomerates is via the single particle mechanism through straining (Table 5b).

With pore throat sizes of 0.4-micron, blockage is through the single pore mechanism accomplished by particle straining (Table 5c).

Conclusion

1. Colloidal particles exist in both treated and untreated produced water and the size distribution of these particles depends on the treatment of the water.
2. Three kinds of particles exist in processed/unprocessed produced water and can be classified as primary, aggregate, and agglomerate particles.
3. Blockage of pore throats is accomplished by either single pore blockage mechanism or through the bridging mechanism.
4. The contribution of primary particles, aggregates, and agglomerates to pore blocking varies depends on the pore throat size, with primary particles and aggregates contributing to blockage through the single pore blocking mechanism while agglomerates block the pore space through the bridging mechanism.
5. This dominant pore throat blocking mechanism (single pore blocking mechanism) is observed across different pore throat sizes, including 0.1, 0.2-, and 0.4-microns pore throat sizes.

Table 4e: Jamming Ratio for particles in Williams County treated produced water on siltstone with d_t = 0.1.

	Pore-throat diameter (d_t) (in microns)	**Particle diameter (d_p) (in microns)**	d_t/d_p
Primary particle (D10)	0.1	2	0.0125
Aggregate (D50)	0.1	35	0.002
Agglomerate (D90)	0.1	150	0.0011

Table 4f: Jamming Ratio for particles in Williams County untreated produced water on siltstone with d_t = 0.2 microns.

	Pore-throat diameter (d_t) (in microns)	**Particle diameter (d_p) (in microns)**	d_t/d_p
Primary particle (D10)	0.2	2	0.1
Aggregate (D50)	0.2	35	0.0057
Agglomerate (D90)	0.2	150	0.0013

Table 4g: Jamming Ratio for particles in Williams County untreated produced water on siltstone with d_t = 0.4 microns.

	Pore-throat diameter (d_t) (in microns)	**Particle diameter (d_p) (in microns)**	d_t/d_p
Primary particle (D10)	0.4	2	0.2
Aggregate (D50)	0.4	35	0.011
Agglomerate (D90)	0.4	150	0.0023

Table 5: Particle size distribution Mountrail County treated produced water.

Parameter	**Value**
MV (µm)	5.26
MN (µm)	3.77
MA (µm)	4.61
CS	1.303
SD	2.053
M_z	5.19
б1	2.002
Ski	0.438
Kg	0.925

6. Pore blockage via bridging mechanism is a rapid process. So, when it is determined that pore-throat blocking via the bridging mechanism can potentially occur, strategies must be put in place to reduce this. Rapid declines in reservoir permeability may also be attributed to this mechanism and this depends on the relationship between the characteristic pore-throat distribution of the reservoir rock and the colloidal particles size distribution in the produced water employed in fracking tight reservoirs.
7. The understanding of these pore blocking mechanisms is crucial for effective reservoir management and can help in designing appropriate strategies to mitigate formation damage.

Acknowledgements

We thank the Department of Petroleum Engineering of the University of North Dakota for providing the produced water samples used in this work. Special thanks go to Dr. James Marti of the University of Minnesota for his technical support in the training required for using the Blue Wave Laser Diffraction equipment. Dr. Kegang Ling's support and the other co-authors in providing advice leading to the organization and writing of this work is equally acknowledged.

Portions of this work were conducted in the Minnesota Nano Center, which is supported by the National Science Foundation through the National Nanotechnology Coordinated Infrastructure (NNCI) under Award Number ECCS - 2025124.

We gratefully acknowledge the help of the North Dakota Industrial Commission for providing financial support to accomplish this work.

Conflict of Interest

There are no conflicts of interest.

Data Availability

The datasets which were generated during this work and supporting its main findings are obtainable from the corresponding author upon reasonable request.

Table 5a: Jamming Ratio for particles in Mountrail treated produced water on siltstone with d_t = 0.1.

	Pore-throat diameter (d_t) (in microns)	Particle diameter (d_p) (in microns)	d_t/d_p
Primary particle (D10)	0.1	5	0.02
Aggregate (D50)	0.1	7	0.0142
Agglomerate (D90)	0.1	8	0.0125

Table 5b: Jamming Ratio for particles in Mountrail treated produced water on siltstone with d_t = 0.2

	Pore-throat diameter (d_t) (in microns)	Particle diameter (d_p) (in microns)	d_t/d_p
Primary particle (D10)	0.2	5	0.04
Aggregate (D50)	0.2	7	0.0285
Agglomerate (D90)	0.2	8	0.025

Table 5c: Jamming Ratio for particles in Mountrail treated produced water on siltstone with d_t = 0.4

	Pore-throat diameter (d_t) (in microns)	Particle diameter (d_p) (in microns)	d_t/d_p
Primary particle (D10)	0.4	5	0.08
Aggregate (D50)	0.4	7	0.0571
Agglomerate (D90)	0.4	8	0.05

References

1. Veil J (2015) U.S. Produced Water Volumes and Management Practices in 2012; Veil Environmental, LLC: Annapolis, MD, USA.
2. Kondash A, Vengosh A (2015) Water footprint of hydraulic fracturing, Environ Sci Technol Lett 2: 276-280.
3. Byrne M, Waggoner S (2009) Fines migration in a high temperature gas reservoir- laboratory simulation and implications for completion design, SPE 121897. Proceeding of the SPE 8th European Formation Damage Conference. Scheveningen, The Netherlands, 27-29 May.
4. Civan F (2007) Reservoir formation damage-fundamentals, modeling, assessment, and mitigation, Gulf Professional Publishing.
5. Hill DG, Lietard OM, Piot BM, et al. (2000) Formation Damage: Origin, Diagnosis and Treatment Strategy. Reservoir Stimulation Book, Third Edition, Chapter 14, John Wiley & Sons, Ltd.
6. Radwan AE, Abudeif A, Attia M, et al. (2019) Development of formation damage diagnosis workflow, application on Hammam Faraun reservoir: A case study, Gulf of Suez, Egypt. In: Offshore Mediterranean Conference. ISBN9788894043679-2019.
7. Radwan AE, Abudeif AM, Attia MM, et al. (2019) Development of formation damage diagnosis workflow, application on Hammam Faraun reservoir: A case study, Gulf of Suez, Egypt. J African Earth Sci 153: 42-53.
8. Radwan AE (2021) Integrated reservoir, geology, and production data for reservoir damage analysis: A case study of the Miocene sandstone reservoir, Gulf of Suez, Egypt. Interpretation 9: 1-46.
9. Fjelde I (2009) Formation damages caused by emulsions during drilling with emulsified drilling fluids. SPE Complete. S2: 222-228.
10. Yang X, Meng Y, Shi X, et al. (2017) Influence of porosity and permeability heterogeneity on liquid invasion in tight gas reservoirs. J Nat Gas Sci Eng 37: 169-177.
11. Katende A, Lu Y, Bunger A, et al. (2020) Experimental quantification of the effect of oil-based drilling fluid contamination on properties of wellbore cement. J Nat Gas Sci Eng 79: 103328.
12. Pang S, Sharma M (1997) In A model for predicting injectivity decline in water-injection wells. SPE 28489, Proceedings of the SPE annual technical conference and exhibition, New Orleans, 25-28.
13. Chequer L, Vaz A, Bedrikovetsky P (2018) Injectivity decline during low salinity waterflooding due to fines migration. Journal of Petroleum Science and Engineering 165: 1054-1072.
14. McDowell-Boyer LM, Hunt JR, Sitar N (1986) Particle transport through porous media. Water Resource Res 22: 1901-1921.
15. Cushing RS, Lawler DF (1998) Depth filtration: Fundamental investigation through three-dimensional trajectory analysis. Environ Sci Technol 32: 3793-3801.
16. Bradford SA, Yates, SR, Bettahar M, et al. (2002) Physical factors affecting the transport and fate of colloids in saturated porous media. Water Resource Res.
17. Bradford SA, Simunek J, Bettahar M, et al. (2003) Modeling colloid attachment, straining, and exclusion in saturated porous media. Environ Sci Technol 37: 2242-2250.
18. Bradford SA, Simunek J, Bettahar M, et al. (2006) Significance of straining in colloid deposition: evidence and implications. Water Resource Res.
19. Shabani A, Zivar D, Jahangiri HR, et al. (2020) Application of pore

network modeling in deep bed filtration analysis. SN Appl Sci 2: 1537.

20. Li X, Scheibe TD, Johnson WP (2004) Apparent decreases in colloid deposition rate coefficient with distance of transport under unfavorable deposition conditions: A general phenomenon. Environ Sci Technol 38: 5616-5625.
21. Ramachandran V, Fogler HS (1999) Plugging by hydrodynamic bridging during flow of stable colloidal particles within cylindrical pores. J Fluid Mech 385: 129-156.
22. Zhang H, Malgaresi GVC, Bedrikovetsky P (2018) Exact solutions for suspension-colloidal transport with multiple capture mechanisms, International Journal of Non-Linear Mechanics 105: 27-42.
23. Kuzmina L, Osipov Y (2019) IOP Conf. Ser.: Mater Sci Eng 661 012122.
24. Tiab D, Donaldson EC, Knovel (2004) Petrophysics: Theory and Practice of Measuring Reservoir Rock and Fluid Transport Properties. Gulf Professional Pub., MA, USA.
25. Watson RB, Viste P, Kaageson-Loe N, et al. (2008) Smart mud filtrate: an engineering solution to minimize near-wellbore formation damage due to kaolinite mobilization, SPE 112455. Proceeding of the SPE International Symposium and Exhibition on Formation Damage Control. Lafayette, Louisiana, USA, 13-15 February.
26. Mungan N (1965) Permeability reduction through changes in pH and salinity. J Petrol Technol 17: 1449-1453.
27. Hergert W, Wriedt T (2012) The Mie Theory: Basics and Applications. Springer.
28. Byrnes AP, Cluff RM (2009) "Analysis of Critical Permeability, Capillary Pressure and Electrical Properties for Mesaverde Tight Gas Sandstones from Western U.S. Basins", Final Report, U.S. Department of Energy contract #DE-FC26-05NT42660, 355.

DOI: 10.36959/901/256